AIAA SciTech Forum
6-10 January 2025, Orlando, FL
AIAA SCITECH 2025 Forum

10.2514/6.2025-1169

Data-Driven Strategy for Enhanced Subgrid Modeling of Reaction-Rate using Linear-Eddy Model for Large Eddy Simulation

A. Panchal[a*], R. Smith[b †], R. Ranjan[b‡] and S. Menon [a§]
[a]*School of Aerospace Engineering, Georgia Institute of Technology*
270 Ferst Drive, Atlanta, GA 30332, USA.
[b]*Department of Mechanical Engineering, The University of Tennessee Chattanooga*
615 McCallie Ave, Chattanooga, TN 37403, USA.

Large eddy simulation (LES) of turbulent combustion requires closure of various subgrid-scale (SGS) terms such as mixing, transport, and chemical reactions. In the present study, we focus on the further assessment and enhancement of the reaction rate closure for LES (RRLES), which utilizes a two-scale strategy. It solves three-dimensional (3D) governing equations for mass, momentum, energy, and species mass and employs the linear-eddy model (LEM) for the subgrid evolution of thermo-chemical quantities to obtain the filtered reaction rate needed by the 3D transport equations. At the subgrid level, before the time-advancement of one-dimensional (1D) LEM equations, the initialization of the thermo-chemical quantities is required, which employed a gradient-based reconstruction strategy in past studies. Such an approach leads to uncertainty within the modeling framework. In the present study, we focus on the assessment of the gradient-based initialization strategy and examine a novel approach for initialization relying on a data-driven convolutional neural network (CNN) strategy. The CNN-based approach utilizes a 3D filtered progress variable field as an input and generates 1D initial conditions for the LEM domain over different filter sizes. For the assessment of the subgrid initialization techniques, we consider a DNS database corresponding to a temporally evolving and freely propagating turbulent premixed flame within the thin reaction zone regime. The results show that in comparison to the gradient-based initialization, the CNN-based initialization leads to reasonable predictions, however, future studies are needed to improve the generalizability of this method for modeling of different regimes and modes of combustion.

I. Introduction

Numerical investigation of turbulent combustion can be performed using approaches with different levels of fidelity. Direct numerical simulation (DNS) is typically used for the investigation of fundamental features of turbulence-chemistry interaction. However, the large computational cost of DNS, particularly while employing finite-rate kinetics, limits its usage to simplified geometries and lower-to-moderate Reynolds number (Re) flows. Large-eddy simulation (LES) appears to be a viable alternative for the simulation of practically relevant flows, where the large scales are resolved, and the effects of subgrid-scale (SGS) are parametrized in terms of closure models.

A particular focus of subgrid modeling in the context of turbulent combustion is on the closure of the highly nonlinear filtered reaction-rate term. For closure of this term [1–3], there exists a wide range of subgrid models (e.g., partially stirred reactor (PaSR) [2], one-dimensional turbulence (ODT) [4], and linear-eddy model (LEM) [5, 6], etc.). Each of these models has their own challenges in terms of its regime of applicability, such as the ability to efficiently account for finite-rate kinetics effects, handling of different modes of turbulent combustion (premixed, non-premixed, partially premixed), issues with low-dimensional manifold-based techniques during extinction/re-ignition dynamics, accounting for inter-scale interactions, etc. The focus here is on subgrid models for finite-rate kinetics, and in particular the multi-scale model RRLES [7], where the subgrid closure of the reaction rate is attained using LEM.

The RRLES approach [7] is a modification of the well-known LEMLES approach [6]. It is a multi-scale strategy that is used to obtain the filtered reaction rate term. The filtered LES equations are evolved on the three-dimensional

[*]Research Engineer II, AIAA Member
[†]Graduate Student, AIAA Member
[‡]Associate Professor, AIAA Senior Member
[§]Professor, AIAA Associate Fellow

(3D) grid and at every time step in a manner similar to a conventional LES and the filtered species mass fractions and the filtered temperature fields are used to reconstruct SGS variation on the 1D notional LEM domain inside each LES cell. After solving for the subgrid reaction-diffusion equation and including the effect of turbulent mixing on the one-dimensional (1D) LEM domain, the filtered reaction rates are computed and projected back to the 3D grid. Since RRLES explicitly models the resolved diffusion and the SGS scalar flux using an eddy-diffusivity approach, the RRLES approach has an advantage over the original LEMLES approach, particularly under a well-resolved or a locally laminar flow condition, and therefore, RRLES can asymptote to the DNS limit. However, it should be noted that the current approach cannot account for counter-gradient transport of scalars, which is often observed in turbulent combustion [8–10], which can be captured by the LEMLES model.

Unlike LEMLES, in the originally proposed RRLES approach, at each time-step, at the subgrid level, the initialization of species mass fraction and temperature fields is performed before they are evolved using LEM. In past studies, the initialization employed the local magnitude of the gradient of these fields following the idea that subgrid 1D LEM lines within a LES cell are notionally oriented along the maximum gradient of the scalar field. Although limited assessment of the initialization approach was performed in past studies, it needs further investigation, and this is a key focus of this study. The sensitivity of initial conditions on 1D LEM calculations is evaluated first. A DNS database of turbulent premixed flame in the thin reaction zone (TRZ) regime [11] is used for this purpose. Sample points within the flame region are selected to extract 1D lines in the flame-normal direction and LEM calculations with these as initial conditions are compared against those with a gradient-based initial condition.

Next, to improve upon the initialization procedure, an initial assessment of a data-driven strategy is considered. We use a convolutional neural network (CNN) that takes the local 3D LES flow-field as inputs and generates 1D initial condition for LEM. CNN is a well-known machine learning (ML) tool that can process and identify key features of images [12] and multi-dimensional data. In terms of combustion applications, CNN has been used to characterize combustion instability [13], detonation mode identification [14], flame detection [15] etc., all using 2D/3D images or flow-fields as inputs. On the other hand, for subgrid modeling of combustion, CNN has been used to predict subgrid flame surface density [16], progress variable variance [17], or flamelet generated manifold [18]. The novelty of this proposed approach is in using finite-rate chemistry (FRC) and LEM with its physics-based reaction-stirring-diffusion modeling for filtered reaction rate computation, while using CNN only for the 1D initialization. Traditional ML-based SGS models are often criticized for their lack of physics awareness and their applicability to conditions/configurations unseen during the training. The current approach aims to address both by coupling CNN with LEM.

This article is arranged as follows. The formulation of RRLES and CNN-based initialization is discussed in Sec. II. In Section **??**, we describe the computational setup and approach considered in this study. The description of results is presented in Sec. IV. Finally, the key outcomes of this study and future outlook are summarized in Sec. V.

II. Mathematical Formulation

Compressible LES equations obtained by spatially filtering the multi-species Navier–Stokes equations using a top-hat Favre filter are used here. Here, $\overline{f}$ is the spatially filtered quantity for a field variable f, and $\widetilde{f} = \overline{\rho f}/\overline{\rho}$ is the Favre-filtered quantity where ρ represents the density. These equations comprise the conservation of mass, momentum, energy, and species mass. For the sake of brevity, these equations are not reported here and can be found elsewhere [7]. In the following text, $(u_i)_{i=1,2,3}$ is the velocity vector in Cartesian coordinates, T is the temperature, P is the pressure, and Y_k is the mass fraction for the k^{th} species. Additionally, N_s is the total number of species in the reacting flow field.

In the formulation considered here, the filtered total energy is presented as a sum of the filtered internal energy ($\widetilde{e}$), the resolved kinetic energy ($0.5[\widetilde{u}_i\widetilde{u}_j]$), and the subgrid kinetic energy ($k^{sgs} = \frac{1}{2}[\widetilde{u_i u_i} - \widetilde{u}_i\widetilde{u}_i]$). All of the subgrid-scale terms in the filtered governing equations require specific modeling. The modeling of subgrid stress and enthalpy flux, subgrid viscous work terms, and the other unclosed subgrid terms in the energy equation is discussed elsewhere [7, 19, 20] and is not the focus here. The focus of the present work is on subgrid modeling of the filtered reaction rate, which is discussed next.

The RRLES approach [7] is a modification of the well-known LEMLES approach [6], where the filtered reaction-rate terms ($\overline{\dot{\omega}}_i$) are modeled using a multi-scale LEM framework. At every LES time step, the filtered species mass fractions ($\tilde{Y}_i$) and the filtered temperature ($\tilde{T}$) evolving at the resolved level are used to reconstruct SGS variation on the 1D notional LEM domain inside each LES cell, and after solving for the subgrid reaction-diffusion equation and including the effect of turbulent mixing on the LEM domain, the filtered reaction rates are computed and projected back to the LES grid. A workflow of the RRLES strategy compared to LEMLES is shown in Fig. 1.

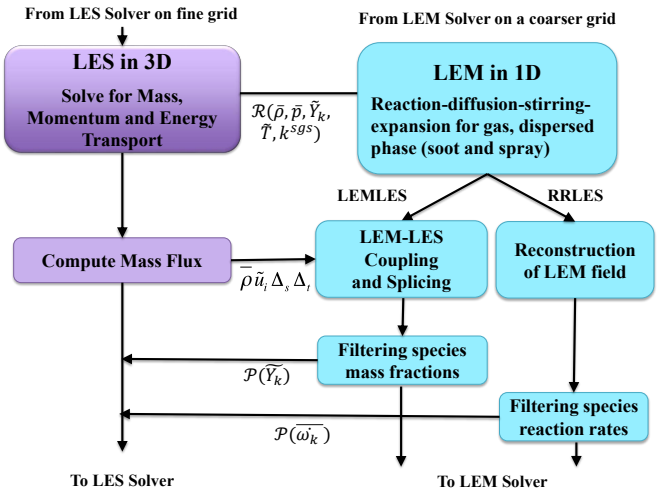

Fig. 1 A typical workflow in the LEMLES and RRLES strategies [7].

The first step in the RRLES modeling strategy is the reconstruction of the species mass fraction and the temperature field in the 1D LEM domain, i.e., setting initial conditions for LEM calculations, which is conventionally performed through

$$Y_i^{\mathrm{LEM}}(s) = \mathcal{R}\left(\widetilde{Y}_i, \nabla\widetilde{Y}_i\right), \quad T^{\mathrm{LEM}}(s) = \mathcal{R}\left(\widetilde{T}, \nabla\widetilde{T}\right), \tag{1}$$

where, conventionally, $\mathcal{R}\left(\widetilde{\phi}, \nabla\widetilde{\phi}\right) = \widetilde{\phi} - |\nabla\widetilde{\phi}|\Delta/2 + |\nabla\widetilde{\phi}|\Delta s$ is a gradient-based reconstruction operator, 's' represents the co-ordinate along the 1D LEM domain, and Δ represents the LES filter size. After the reconstruction step, the governing equations for the species mass-fraction and the temperature are solved on the notional 1D LEM domain inside each LES computational cell as

$$\rho\frac{\partial Y_i}{\partial t} = F_{i,\mathrm{stir}} - \frac{\partial}{\partial s}\left(\rho Y_i V_{s,i}\right) + \dot{\omega}_i, \tag{2}$$

$$\rho C_{p,\mathrm{mix}}\frac{\partial T}{\partial t} = F_{T,\mathrm{stir}} + \frac{\partial}{\partial s}\left(\kappa\frac{\partial T}{\partial s}\right) - \frac{\partial}{\partial s}\left(\sum_{i=1}^{N_S} h_i \rho Y_i V_{s,i}\right) - \sum_{i=1}^{N_S} h_i \dot{\omega}_i. \tag{3}$$

Each 1D LEM domain is discretized using N_{LEM} cells to ensure the required spatial resolution of the scalar fields. The processes involved in the subgrid evolution include molecular diffusion, turbulent transport by the unresolved eddies, chemical reaction, and thermal expansion for the species at their respective spatial and temporal scales. The terms $F_{k,\mathrm{stir}}$ and $F_{T,\mathrm{stir}}$ represent the stochastic events, which simulate the effects of turbulent mixing by the SGS eddies on the 1D LEM lines [6, 21]. Finally, after solving for the subgrid fields (species mass fraction and temperature), the filtered reaction-rate term $\overline{\dot{\omega}}_i$ is obtained for the corresponding LES cell through:

$$\overline{\dot{\omega}}_i = \frac{\sum_{m=1}^{N_{\mathrm{LEM}}} \dot{\omega}_{i,m}\Delta V_m}{\sum_{m=1}^{N_{\mathrm{LEM}}} \Delta V_m}. \tag{4}$$

The approach was extended to use a single grid-based strategy to enable the application to complex geometries [22]. Recently, a local dual grid-based strategy has also been developed, which can potentially be used with different grid topologies, without the need for an AMR [11, 23].

As noted earlier, initialization (also referred to as reconstruction $\mathcal{R}$) of the 1D LEM domain ($Y_i^{\mathrm{LEM}}(s)$, $T^{\mathrm{LEM}}(s)$) is conventionally handled using maximum scalar gradients computed on the LES grid. This traditional initialization is shown in Eq. 1, but its accuracy and sensitivity to LEM calculations are not clear yet and are the focus of this work. The proposed strategy for initialization with CNN is shown in Fig. 2. The 3D LES field surrounding the target location is used as an input to the CNN. The CNN outputs the 1D LEM initialization for scalars and temperature. This is then used to evolve the LEM (Eq. 2- 3), and the filtered reaction rate is computed after the evolution as shown in Eq. 4.

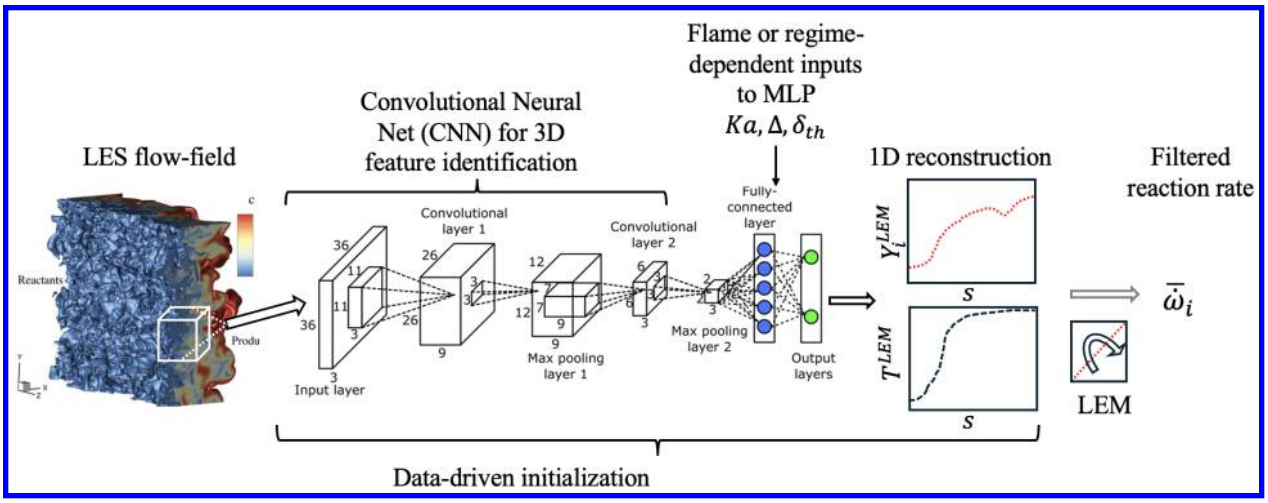

Fig. 2 Schematic of the CNN approach for reconstruction on 1D LEM domain for reaction rate closure. The data-driven strategy uses CNN for 3D feature identification and this is followed by a fully-connected multi-layer perceptron (MLP) network that has additional inputs corresponding to the combustion regime and conditions, e.g., Karlovitz number Ka, thermal flame thickness δ_{th}, and LES filter width Δ.

III. Computational Approach

A schematic of the canonical turbulent premixed flame setup is shown in Fig. 3. This test case corresponds to a freely propagating methane/air turbulent premixed flame configuration where an initially one-dimensional (1D) planar laminar methane/air premixed flame interacts with a decaying background isotropic turbulence. The setup follows past studies, which have focused on the investigation of fundamental aspects of flame-turbulence interactions and to assess the capabilities of novel computational methods and models [7, 22, 24–26]. The computational domain comprises a 3D cube with the length of the side denoted by L. The initial planar flame is specified to be near the center of the computational domain with the reactants on the left side and the products on the right side of the domain. The initial isotropic turbulence is obtained by evolving the flow field specified using the Kraichnan spectrum [27] and re-scaling the evolved velocity field to match the desired turbulence intensity (u'). The value of $L = 0.006$ is chosen to ensure that $L/l \geq 10$, where l is the initial value of the integral length scale of the initial isotropic turbulent flow. The initial flow field is superimposed with the 1D laminar premixed flame solution obtained at $\phi = 0.8$, $T_{\text{ref}} = 570$ K and $P_{\text{ref}} = 1$ atm. Here, ϕ, T_{ref}, P_{ref} denote the equivalence ratio, temperature on the unburnt reactants side, and reference pressure, respectively. The flame conditions, particularly the preheated conditions and the equivalence ratio, chosen here are nominally based on past studies and are typical of gas turbines, spark-ignition engines, and combustors [24, 28]. Based on the initial conditions, the flame corresponds to the thin reaction zone (TRZ) regime [8] with $u'/S_{\text{L}} = 10$ and $l/\delta_{\text{L}} = 1.87$. Here, S_{L} and $\delta_{\text{L}} = (T_{\text{b}} - T_{\text{u}})/|\nabla T|_{\text{max}}$ denote the laminar flame speed and laminar flame thickness, respectively. The subscripts 'b' and 'u' denote burnt and unburnt regions, respectively.

A characteristic-based inflow-outflow boundary condition is used in the streamwise (x) direction and a periodic boundary condition is used in the homogeneous transverse (y) and spanwise (z) directions. The computational domain for DNS is spatially discretized using a uniformly spaced grid of size $256 \times 256 \times 256$. The simulations are carried out up to $t/t_0 = 3$ to allow for spatio-temporal evolution of flame-turbulence interactions. Here, $t_0 = l/u'$ is the initial eddy turnover time. Although turbulence decays with time in this case, however, flame-turbulence interactions attain a nearly quasi-stationary state within one or two eddy-turnover times [7, 25, 26], and therefore, such interactions can be examined during such stage. The DNS data from this setup is then used for studying the sensitivity of initial conditions on 1D LEM calculations at sample locations.

The governing equations described earlier are solved using a well-established three-dimensional (3D) parallel, multi-species compressible reacting flow solver, referred to as AVF-LESLIE [24, 29]. It is a multi-physics simulation tool capable of performing DNS and LES of reacting/non-reacting flows in canonical and moderately complex flow configurations. It has been extensively used in the past to study a wide variety of flow conditions, including acoustic flame-vortex interaction, premixed flame turbulence interaction, and non-premixed combustion. [24, 26, 29, 30].

The solver utilizes a finite volume-based spatial discretization of the governing equations in their conservative form

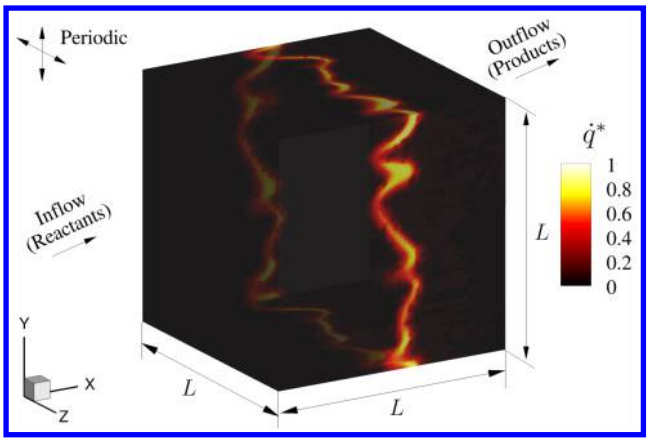

Fig. 3 Schematic of the turbulent premixed flame test case considered in the present study.

on a structured grid using the generalized curvilinear coordinates. The spatial discretization is based on the well-known second-order accurate MacCormack scheme [31]. The time integration of the semi-discrete system of equations is performed by an explicit second-order accurate scheme. The solver can handle arbitrarily complex finite-rate chemical kinetics. The mixture-averaged transport properties, the finite-rate kinetics source terms, and the thermally perfect gas-based thermodynamic properties are obtained using the Cantera software. The parallelization of the solver is based on the standard domain decomposition technique based on the message-passing interface library.

IV. Results

The DNS dataset of the turbulent premixed flame case is used to perform an *a priori* analysis. We utilize different top-hat kernels corresponding to 8, 16, 24, 32, 40, and 48 times the DNS grid resolution (along one direction) for generating a filtered flow field from the DNS data. Approximately 100 sample points in the flame region are chosen for the analysis. For each point, the flame-normal direction is determined and temperature and species concentration data is extracted along this direction to generate the 'true' initial conditions for the 1D LEM calculations. These are compared against the conventional gradient-based initial conditions generated using a filtered solution. Corresponding results for a representative location in the flame region are shown in Fig. 4. We can observe that for small filter sizes, i.e., closer to the DNS grid resolution, the gradient-based reconstruction matches reasonably well with the DNS-extracted solution. However, for filters coarser than 16X, significant errors are observed since the DNS-extracted solution shows a near hyperbolic tangent profile with the flame located near the center while the gradient-based reconstruction fails to capture this.

These initial conditions are next used for 1D LEM calculations, and the results are shown in Fig. 5. The presented results are for the same representative point in the flame region, however, multiple realizations are conducted as LEM is a stochastic approach. The results are presented for different filter widths, and use corresponding subgrid Reynolds number $Re_\Delta = u'\Delta/\nu$ with $u' = \sqrt{2k_{sgs}}$ as the subgrid velocity fluctuation, Δ as the filter width, and ν as the kinematic viscosity as an input. The LEM calculations are conducted for a 2 μs window starting from the initial conditions and this represents a typical CFL-based time-step for LES simulations. The reaction rate and mass fraction of CH_4 and temperature fields are representatively shown.

We can observe that the results match well for the 8X filtering between the gradient-based reconstruction and the DNS-extracted initial conditions. However, significant differences are noted for larger filter sizes. For example, at 32X filter size, flame-like features defined by a peak in the reaction rate in the center and temperature increase towards the products are observed for the DNS-extracted initial conditions, but not for the gradient-based reconstruction. These results suggest that the gradient-based reconstruction can be a reasonable approximation for finer LES grids but not for larger filter sizes. This is further evident from Fig. 6 where the predicted filtered reaction rates from the LEM calculation (using Eq. 4) are compared for different species. A reasonable match is obtained for a smaller filter size between the gradient-based reconstruction and the DNS-extracted initial conditions, however, significant differences are observed for filters coarser than 24X. Note that the performance of 1D LEM tends to be better when there is significant

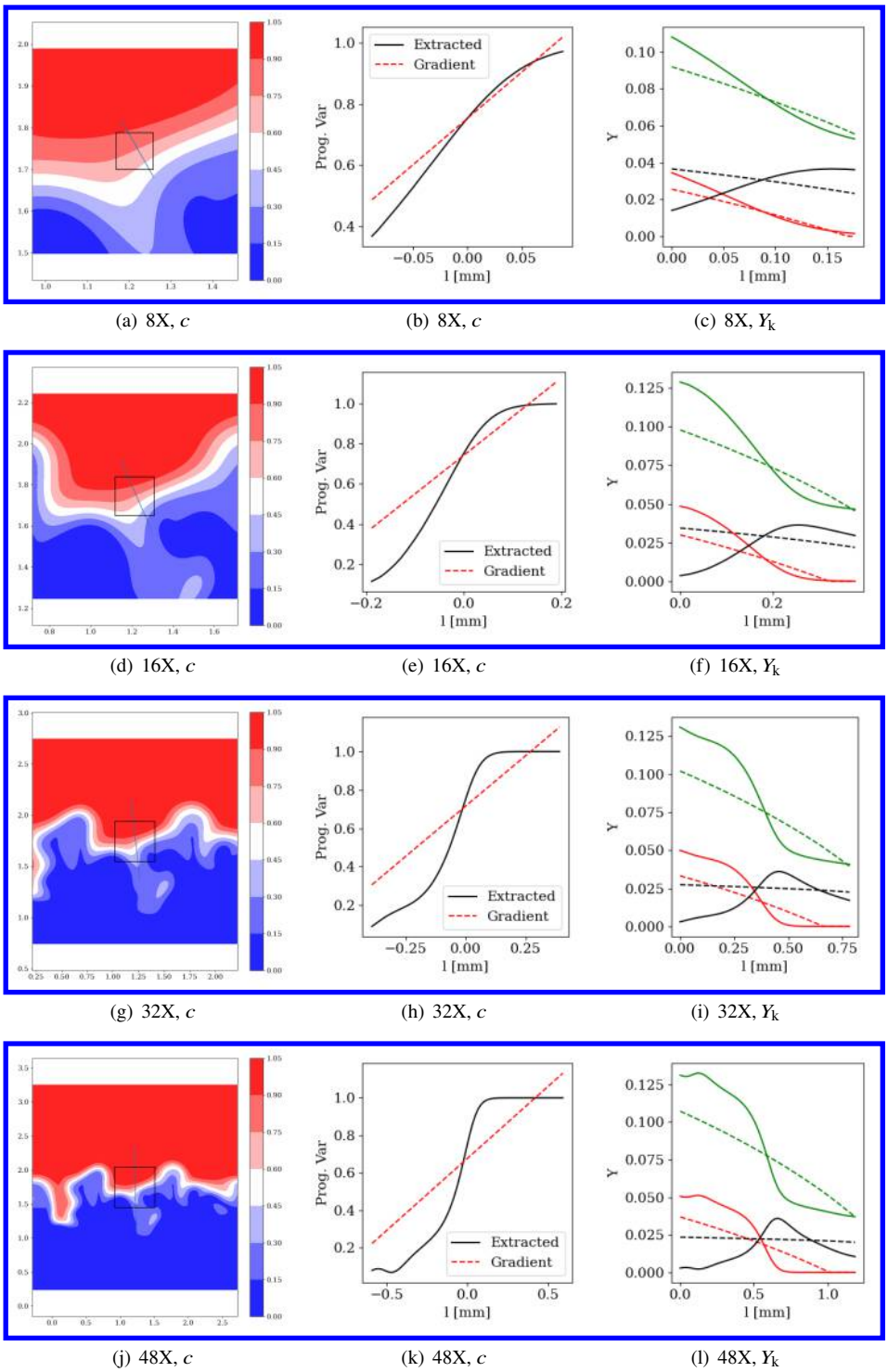

(a) 8X, c (b) 8X, c (c) 8X, Y_k

(d) 16X, c (e) 16X, c (f) 16X, Y_k

(g) 32X, c (h) 32X, c (i) 32X, Y_k

(j) 48X, c (k) 48X, c (l) 48X, Y_k

Fig. 4 Comparison of gradient-based initial conditions against DNS-extracted data along a 1D line normal to the flame direction for a sample point in the flame. The first column shows the progress variable (c) field from DNS centered around the sample point of analysis. The filtered cell is shown as a box with black outline. The 1D line normal to the flame-front is shown in blue. The comparison of extracted values and gradient-based reconstruction of progress variable is shown in the second column. The third column compares species mass fractions of CH_4 (red), O_2 (green) and CO (black) between gradient-based reconstruction (dashed) and DNS (solid). The rows correspond to different filtering sizes from 8X to 48X.

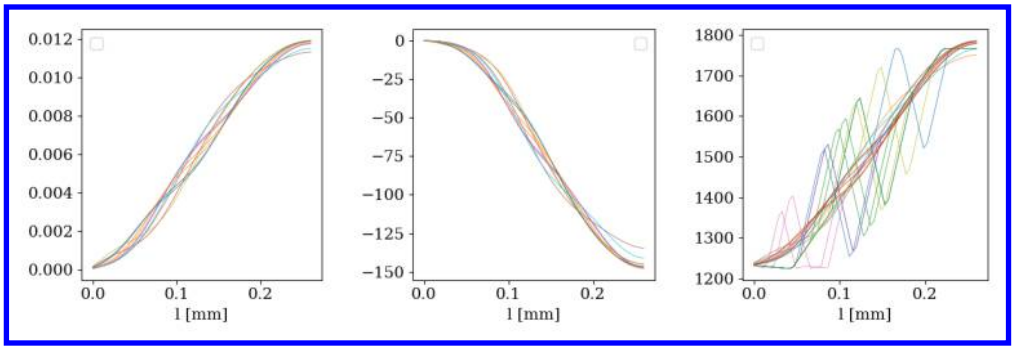

(a) 8X, Y_{CH_4}, Gradient (b) 8X, $\dot{\omega}_{CH_4}$, Gradient (c) 8X, T, Gradient

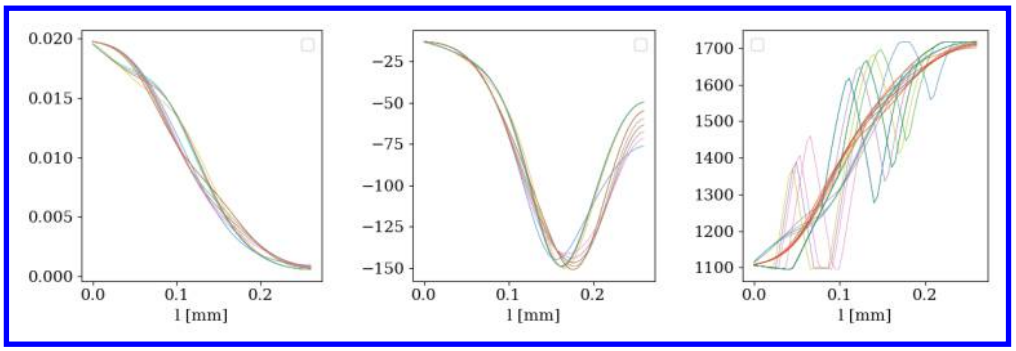

(d) 8X, Y_{CH_4}, Extracted (e) 8X, $\dot{\omega}_{CH_4}$, Extracted (f) 8X, T, Extracted

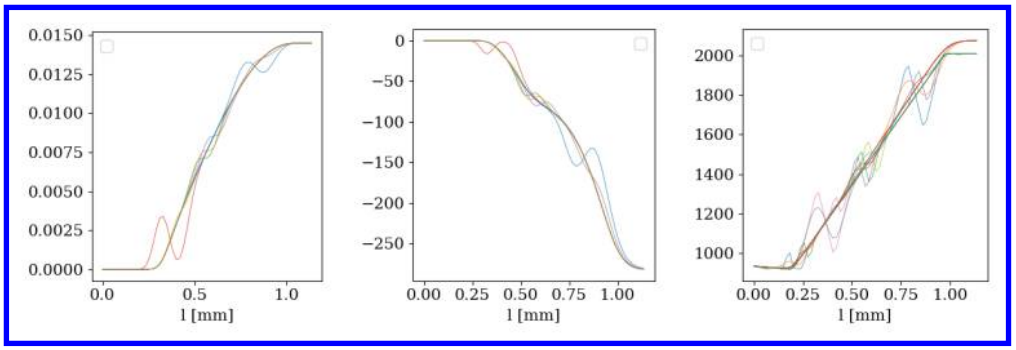

(g) 32X, Y_{CH_4}, Gradient (h) 32X, $\dot{\omega}_{CH_4}$, Gradient (i) 32X, T, Gradient

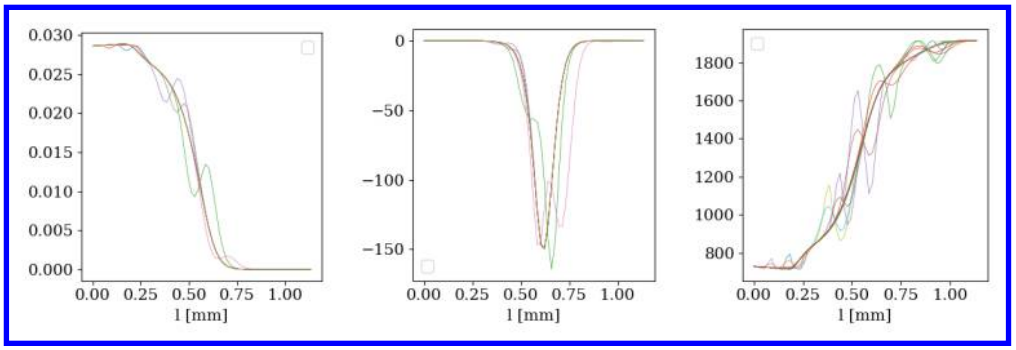

(j) 32X, Y_{CH_4}, Extracted (k) 32X, $\dot{\omega}_{CH_4}$, Extracted (l) 32X, T, Extracted

Fig. 5 Resulting CH_4 mass fraction (Y_{CH_4}), reaction rate ($\dot{\omega}_{CH_4}$) [kg/m3/s], and temperature (T) [K] from gradient-based and DNS-extracted initial conditions after LEM calculations for 2 μs. The rows correspond to different filtering sizes from 8X to 48X. Different lines correspond to different realizations starting from the same initial condition.

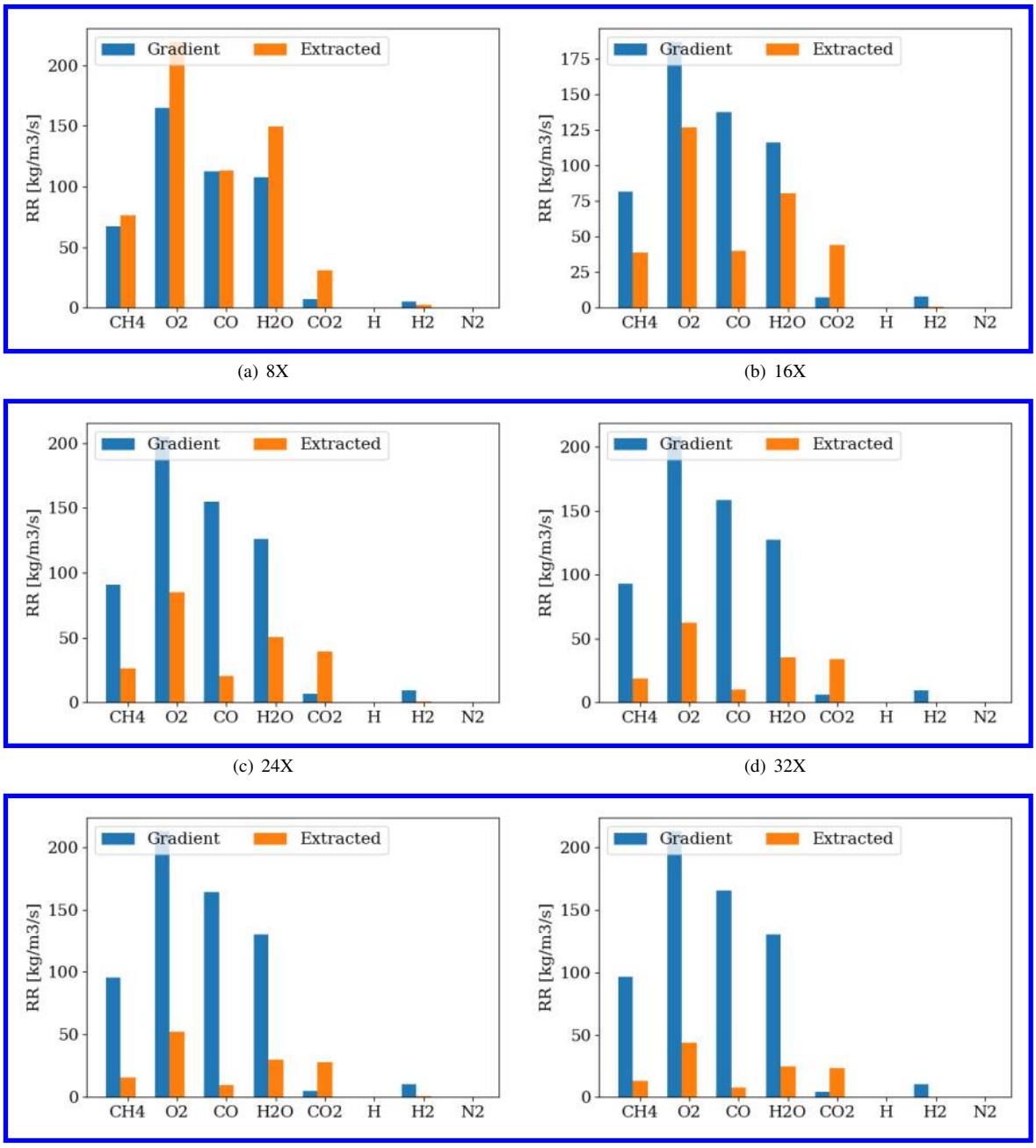

(a) 8X (b) 16X

(c) 24X (d) 32X

(e) 40X (f) 48X

Fig. 6 Estimated filtered reaction rates (RR [kg/m3/s]) of different species from the 1D LEM calculations are compared starting from gradient-based vs. DNS-extracted initial conditions. Results are shown for different filter sizes.

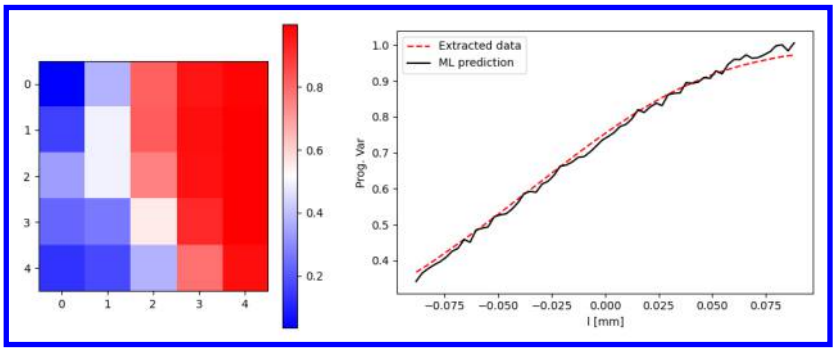

(a) 8X, Input Prog. Var (b) 8X, Prediction

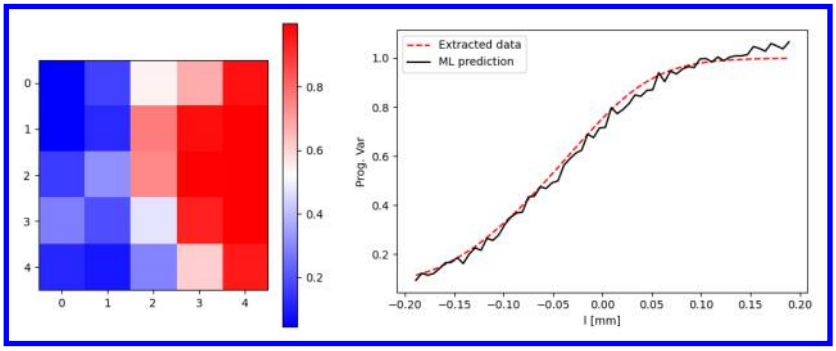

(c) 16X, Input Prog. Var. (d) 16X, Prediction

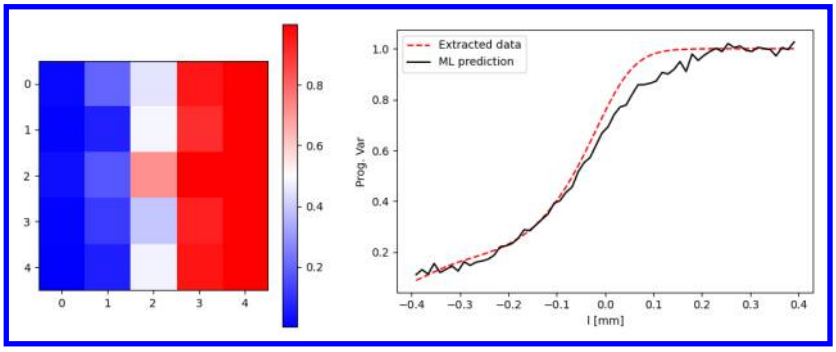

(e) 32X, Input Prog. Var. (f) 32X, Prediction

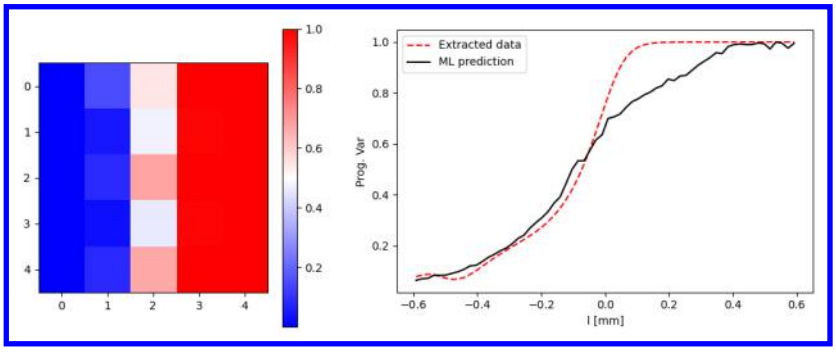

(g) 48X, Input Prog. Var. (h) 48X, Prediction

Fig. 7 Inputs to the machine learning model, i.e., LES-filtered progress variable flow-field (first column), and predicted output, i.e., 1D initial conditions to be used for LEM calculation (second column) are shown for different filter sizes as an initial assesment of the ML model. The DNS-extracted data (dashed line) is shown as reference.

subgrid variation, which implies the need to have a coarser LES grid [7]. These results highlight the need to improve the initialization strategy, particularly, while employing coarser grids for LES.

Considering the need for physically accurate initial conditions for subgrid LEM calculations, a preliminary assessment of the aforementioned machine learning (ML) approach is conducted next. The machine learning approach is trained using 100 randomly selected points in the flame region from the turbulent premixed flame DNS database and for different filter sizes. The filtered progress variable flow field is used as an input (as this is usually available in LES simulations) and the output is the 1D variation of progress variable, temperature, and species mass fractions along the flame-normal direction. The ML predictions for the same representative point discussed earlier are shown in Fig. 7 across different filter sizes. The ML model follows the DNS-extracted 'truth' solution reasonably well up to 32X filter size and shows an improvement over the gradient-based reconstruction discussed so far. It is noted that the current results serve only as an initial assessment of the data-driven approach and future work will evaluate the generalizability of this approach over a range of conditions, e.g., different Karlovitz numbers, and for non-premixed and partially premixed combustion.

V. Conclusions

The present study focuses on the assessment of an enhanced subgrid model relying on LEM for the filtered reaction rate. The model, referred to as RRLES, utilizes a multi-scale framework, where the reacting flow field is evolved on a conventional LES grid, while the filtered reaction rate is obtained by evolving LEM equations at the subgrid level. The subgrid evolution requires initialization of the scalar fields on the LEM domain. Using a DNS dataset of turbulent premixed flame operating in the thin reaction zone (TRZ) regime, this work evaluates the effect of initial conditions on subgrid LEM calculations.

The subgrid LEM initial conditions are conventionally constructed using a linear reconstruction based on large-scale gradients. As a first step, this approach is compared against progress variable, temperature, and species mass fraction data extracted along the flame-normal direction from the DNS at different filter sizes. The results match well for smaller filter sizes, i.e., closer to the DNS resolution, however, significant differences are observed for filter sizes beyond 32X. These initial conditions are then used for LEM calculations to evaluate the sensitivity of initial conditions on predicted reaction rates. The reaction rates computed from LEM between the gradient-based and DNS-extracted initial conditions match well for 8X filter size but not for filters coarser than that and this suggests the need for a better approach to generate initial conditions for subgrid LEM while using a RRLES approach.

To this extent, an initial assessment of a data-driven ML strategy is considered. A convolutional neural net (CNN) is used here that takes the filtered 3D progress variable field as an input to predict the 1D initial conditions to be used on the LEM domain. The current ML predictions match reasonably well with the DNS-extracted 'truth' solution, however, further study is needed to test the generalizability of this approach and then couple it with LES simulations. To analyze the generalizability of the proposed approach, a higher turbulence condition on which the model is not trained on and non-premixed flames will be considered in the future.

Acknowledgment

Dr. Ranjan acknowledges the National Science Foundation (NSF) (Grant #: 2301829 , Program Officer: Dr. Harsha Chelliah) for partly supporting this work. The computational resources provided by the UTC Research Institute through NSF Grants Nos. 1925603 and 2201497 are greatly appreciated.

References

[1] Pitsch, H., "Large-eddy simulation of turbulent combustion," *Annu. Rev. Fluid Mech.*, Vol. 38, 2006, pp. 453–482.

[2] Fureby, C., "Large eddy simulation modelling of combustion for propulsion applications," *Philosophical Transactions of the Royal Society A: Mathematical, Physical and Engineering Sciences*, Vol. 367, No. 1899, 2009, pp. 2957–2969.

[3] Gonzalez-Juez, E. D., Kerstein, A. R., Ranjan, R., and Menon, S., "Advances and challenges in modeling high-speed turbulent combustion in propulsion systems," *Prog. Energy Combust. Sci.*, Vol. 60, 2017, pp. 26–67.

[4] Echekki, T., Kerstein, A. R., Dreeben, T. D., and Chen, J.-Y., "?One-dimensional turbulence? simulation of turbulent jet diffusion flames: model formulation and illustrative applications," *Comp. and Fluids*, Vol. 125, No. 3, 2001, pp. 1083–1105.

[5] Menon, S., McMurtry, P., and Kerstein, A. R., "A Linear Eddy Mixing Model for Large Eddy Simulation of Turbulent

Combustion," *LES of Complex Engineering and Geophysical Flows*, edited by B. Galperin and S. Orszag, Cambridge University Press, 1993, pp. 287–314.

[6] Menon, S., and Kerstein, A. R., "The linear-eddy model," *Turbulent Combustion Modeling*, Vol. 95, 2011, pp. 175–222.

[7] Ranjan, R., Muralidharan, B., Nagaoka, Y., and Menon, S., "Subgrid-Scale Modeling of Reaction-Diffusion and Scalar Transport in Turbulent Premixed Flames," *Combust. Sci. Technol.*, Vol. 188, 2016, pp. 1496–1537.

[8] Peters, N., *Turbulent Combustion*, Cambridge University Press, 2000.

[9] Swaminathan, N., Bilger, R., and Cuenot, B., "Relationship between turbulent scalar flux and conditional dilatation in premixed flames with complex chemistry," *Comp. and Fluids*, Vol. 126, No. 4, 2001, pp. 1764–1779.

[10] Veynante, D., Trouve, A., Bray, K. N. C., and Mantel, T., "Gradient and counter-gradient scalar transport in turbulent premixed flames," *J. Fluid Mech.*, Vol. 332, 1997, pp. 263–293.

[11] Smith, R., Elliott, T., and Ranjan, R., "Subgrid modeling of reaction-rate using a multi-scale strategy for large-eddy simulation of turbulent combustion," *Thermal and Fluids Engineering Conference*, American Society of Thermal and Fluid Engineers, 2024.

[12] Gu, J., Wang, Z., Kuen, J., Ma, L., Shahroudy, A., Shuai, B., Liu, T., Wang, X., Wang, G., Cai, J., et al., "Recent advances in convolutional neural networks," *Pattern recognition*, Vol. 77, 2018, pp. 354–377.

[13] Gangopadhyay, T., Locurto, A., Boor, P., Michael, J. B., and Sarkar, S., "Characterizing combustion instability using deep convolutional neural network," *Dynamic Systems and Control Conference*, Vol. 51890, American Society of Mechanical Engineers, 2018, p. V001T13A004.

[14] Johnson, K. B., Ferguson, D. H., Tempke, R. S., and Nix, A. C., "Application of a convolutional neural network for wave mode identification in a rotating detonation combustor using high-speed imaging," *Journal of Thermal Science and Engineering Applications*, Vol. 13, No. 6, 2021, p. 061021.

[15] Zhong, Z., Wang, M., Shi, Y., and Gao, W., "A convolutional neural network-based flame detection method in video sequence," *Signal, Image and Video Processing*, Vol. 12, 2018, pp. 1619–1627.

[16] Lapeyre, C. J., Misdariis, A., Cazard, N., Veynante, D., and Poinsot, T., "Training convolutional neural networks to estimate turbulent sub-grid scale reaction rates," *Combustion and Flame*, Vol. 203, 2019, pp. 255–264.

[17] Xing, V., Lapeyre, C., Jaravel, T., and Poinsot, T., "Generalization capability of convolutional neural networks for progress variable variance and reaction rate subgrid-scale modeling," *Energies*, Vol. 14, No. 16, 2021, p. 5096.

[18] Seltz, A., Domingo, P., Vervisch, L., and Nikolaou, Z. M., "Direct mapping from LES resolved scales to filtered-flame generated manifolds using convolutional neural networks," *Combustion and Flame*, Vol. 210, 2019, pp. 71–82.

[19] Menon, S., and Kim, W., "High Reynolds number flow simulations using the localized dynamic subgrid-scale model," *AIAA paper*, Vol. 425, 1996, p. 1996.

[20] Kim, W. W., and Menon, S., "An unsteady incompressible Navier-Stokes solver for large eddy simulation of turbulent flows," *I. J. for Numer. Meth. Fluids.*, Vol. 31, No. 6, 1999, pp. 983–1017.

[21] Kerstein, A. R., "Linear-eddy modeling of turbulent transport. II: Application to shear layer mixing," *Combust. Flame*, Vol. 75, No. 3-4, 1989, pp. 397–413.

[22] Panchal, A., Ranjan, R., and Menon, S., "A comparison of finite-rate kinetics and flamelet-generated manifold using a multiscale modeling framework for turbulent premixed combustion," *Combustion Science and Technology*, Vol. 191, No. 5-6, 2019, pp. 921–955.

[23] Ranjan, R., "A dual grid strategy for subgrid reaction-rate closure using linear eddy mixing model for large-eddy simulation of turbulent combustion," *APS Division of Fluid Dynamics Meeting Abstracts*, 2021, pp. H09–003.

[24] Sankaran, V., and Menon, S., "Subgrid combustion modeling of 3-D premixed flames in the thin-reaction-zone regime," *Proc. Combust. Inst.*, Vol. 30, No. 1, 2005, pp. 575–582.

[25] Savre, J., Carlsson, H., and Bai, X. S., "Turbulent methane/air premixed flame structure at high Karlovitz numbers," *Flow Turbulence Combust.*, Vol. 90, No. 2, 2013, pp. 325–341.

[26] Bowers, J., Durant, E., and Ranjan, R., "Effects of Pressure and Characteristic Scales on the Structural and Statistical Features of Methane/Air Turbulent Premixed Flames," *Flow, Turbulence and Combustion*, 2024, pp. 1–37.

[27] Kraichnan, R. H., "Diffusion by a random velocity field," *Phys. of Fluids*, Vol. 13, No. 1, 1970, pp. 22–31.

[28] Sankaran, R., Hawkes, E. R., Chen, J. H., Lu, T., and Law, C. K., "Structure of a spatially developing turbulent lean methane–air Bunsen flame," *Proc. Combust. Inst.*, Vol. 31, No. 1, 2007, pp. 1291–1298.

[29] Kim, W.-W., and Menon, S., "Numerical modeling of turbulent premixed flames in the thin-reaction-zones regime," *Combust. Sci. Technol.*, Vol. 160, No. 1, 2000, pp. 119–150.

[30] Yang, S., Ranjan, R., Yang, V., Wenting, S., and Menon, S., "Sensitivity of predictions to chemical kinetics models in a temporally evolving turbulent non-premixed flame," *Combustion and Flame*, Vol. 183, 2017, pp. 224–241.

[31] MacCormack, R. W., "The effect of viscosity in hypervelocity impact cratering," *J. Space. Rockets*, Vol. 40, No. 5, 2003, pp. 757–763.